JOURNAL OF VIROLOGY, July 2010, p. 7064–7072 Vol. 84, No. 14
0022-538X/10/$12.00 doi:10.1128/JVI.02400-09

Merkel Cell Polyomavirus-Infected Merkel Cell Carcinoma Cells Require Expression of Viral T Antigens▽

Roland Houben,[1]† Masahiro Shuda,[2]† Rita Weinkam,[1] David Schrama,[1] Huichen Feng,[2] Yuan Chang,[2]*‡ Patrick S. Moore,[2]*‡ and Jürgen C. Becker[1]‡

Department of Dermatology, Julius Maximilians University, Würzburg, Germany,[1] and Molecular Virology Program, University of Pittsburgh Cancer Institute, Pittsburgh, Pennsylvania 15213[2]

Received 13 November 2009/Accepted 25 April 2010

Merkel cell carcinoma (MCC) is the most aggressive skin cancer. Recently, it was demonstrated that human Merkel cell polyomavirus (MCV) is clonally integrated in ~80% of MCC tumors. However, direct evidence for whether oncogenic viral proteins are needed for the maintenance of MCC cells is still missing. To address this question, we knocked down MCV T-antigen (TA) expression in MCV-positive MCC cell lines using three different short hairpin RNA (shRNA)-expressing vectors targeting exon 1 of the TAs. The MCC cell lines used include three newly generated MCV-infected cell lines and one MCV-negative cell line from MCC tumors. Notably, all MCV-positive MCC cell lines underwent growth arrest and/or cell death upon TA knockdown, whereas the proliferation of MCV-negative cell lines remained unaffected. Despite an increase in the number of annexin V-positive, 7-amino-actinomycin D (7-AAD)-negative cells upon TA knockdown, activation of caspases or changes in the expression and phosphorylation of Bcl-2 family members were not consistently detected after TA suppression. Our study provides the first direct experimental evidence that TA expression is necessary for the maintenance of MCV-positive MCC and that MCV is the infectious cause of MCV-positive MCC.

Merkel cell carcinoma (MCC) is a highly aggressive neuroendocrine skin cancer. Although it is rare, its reported incidence is increasing (19). MCC is associated with UV exposure and affects primarily elderly and immune-suppressed patients (5, 11, 17, 26). The susceptibility of MCC to immune surveillance is similar to that of known virus-induced cancers and suggests that MCC has an infectious trigger (9). Recently, a new human polyomavirus, termed Merkel cell polyomavirus (MCV), was discovered to be clonally integrated into MCC tumor genomes (14). While MCV integration occurs at distinct sites in MCC tumors from different individuals, primary tumors and corresponding metastases have identical integration sites, consistent with the occurrence of MCV infection and integration prior to clonal expansion and metastasis (14, 37). A number of studies have confirmed that MCV is present in 69 to 85% of MCC tumors collected from Europe and the United States (4, 15, 21, 41). Surveys of control non-MCC skin, hematolymphoid, and neuroendocrine tumors are generally negative for MCV, although incidental low-level infection can be detected (4, 14, 22, 33, 34, 39, 42, 44).

All polyomaviruses encode alternatively spliced large T (LT) and small T (sT) antigen transcripts that share exon 1 of the T-antigen (TA) locus. Additional multiply spliced TA transcripts have been described for different polyomaviruses, including the 17kT and 57kT antigens in simian virus 40 (SV40) and MCV, respectively (40, 46). Research on viral proteins encoded by the TA locus has been central to uncovering cell signaling networks important in cancer biology (10, 38). The targeting of cellular proteins, such as retinoblastoma protein (Rb), p53, and protein phosphatase 2A (PP2A), by TAs contributes to polyomavirus-induced cell transformation (for reviews, see references 1 and 2). MCV TAs that are expressed in MCC tumors lack a putative p53 binding domain because of tumor-associated T-antigen deletion mutations (37, 40). Other conserved tumor suppressor-targeting motifs, including the Rb binding domain (LXCXE motif), the J domain (HPDK) in LT/57kT, and a putative PP2A interaction domain in sT, remain intact (40).

Current data point toward MCV as the infectious cause for most Merkel cell cancers: the virus is associated with MCC tumors and, when present, expresses T antigen in tumor cells but not in healthy surrounding tissues (7, 20, 39). MCV is specific to MCC and is not detected at significant levels in other cancers or in healthy skin examined to date, despite widespread circulation of MCV among human populations (8, 23, 29, 42). Clonal analysis of MCC tumors also supports the correct temporal relationship for causality; i.e., MCV infection occurs prior to MCC tumor development (18). If MCV is a direct cause of MCC tumorigenesis, it is expected that MCC tumors will require MCV protein expression to maintain the tumor phenotype—the so-called oncogene addiction.

To address this question, we generated four new MCC cell lines that were examined together with previously established MCC and non-MCC cell lines. Using two independent methods, we show that short hairpin RNA (shRNA) targeting of the MCV T antigens initiates cell cycle arrest and cell death only in MCV-positive MCC cells. Thus, MCV TA expression is nec-

* Corresponding author. Mailing address: Molecular Virology Program, University of Pittsburgh Cancer Institute, 5117 Centre Ave., Pittsburgh, PA 15213. Phone: (412) 623-7721. Fax: (412) 623-7715. E-mail for Yuan Chang: yc70@pitt.edu. E-mail for Patrick S. Moore: psm9@pitt.edu.
† R.H. and M.S. contributed equally to this work.
‡ Y.C., P.S.M., and J.C.B. are co-senior authors of this paper.
▽ Published ahead of print on 5 May 2010.

TABLE 1. MCC cell lines used in this study

Cell line	Source			Morphology	Doubling time (days)	Detection of MCV by:		LT		Expression[a] of:				
	Age of patient[b]	Sex of patient[b]	Location			PCR	Southern blotting	Stop codon mutation[c]	Predicted molecular mass (kDa)	CK-20	Pan-CK	NSE	Chromogranin A	Synaptophysin
UISO	46	F	Thigh	Adherent	1.5	−	−	NA	NA	−	ND	++	−	−
MCC13	80	F	Nodal metastasis[d]	Adherent	1	−	−	NA	NA	−	−	+	+	−
MaTi	88	F	Lymph node metastasis	Spheroidal	2.5	−	−	NA	NA	−	−	+	−	−
MKL-1	26	M	Nodal metastasis[e]	Spheroidal	3	+	+	Deletion, nt 1612-1657[f]	36	+	+	++	+	+
WaGa	67	M	Ascites	Single cell suspension	4	+	ND	C1461T	30	+	+	+	+	+
BroLi[g]	55	M	Pleural effusion	Spheroidal	5	+	ND	ND	ND	+	+	++	+	+
MS-1	59	F	Adrenal metastasis	Spheroidal	4	+	+	Deletion, nt 1912-1951	47	+	+	+	+	+
MKL-2	72	M	ND	Spheroidal	5	+	+	C1453A	30	+	ND	ND	+	+

[a] Expression of cytokeratin-20 (CK-20), pan-cytokeratin (pan-CK), neuron-specific enolase (NSE), and Ki-67 was measured by immunocytochemistry. Synaptophysin and chromogranin A expression was analyzed by quantitative real-time PCR.
[b] See reference 35 for UISO, reference 42a for MKL-2, reference 27 for MCC13, and reference 40 for MKL-1.
[c] Identified by sequencing of PCR amplicons. NA, not applicable. ND, not determined or unknown.
[d] See reference 2.
[e] See reference 3.
[f] See reference 45.
[g] For the BroLi cell line, we were not able to amplify the complete TA gene. While PCR amplicons spanning nucleotides 196 to 1428 of the MCV genome (GenBank accession no. EU375803) could be generated, PCR using a multitude of different primer pairs located outside this region did not yield products. Immunoblotting, however, demonstrates that in BroLi, LT is truncated in a manner typical of MCC (Fig. 2).

essary to maintain the oncogenic phenotype of MCV-positive MCC cell lines.

MATERIALS AND METHODS

Ethics statement. This study analyzing human cell lines was conducted according to the principles expressed in the Declaration of Helsinki. The study was approved by the Institutional Review Board of Würzburg University Hospital (Ethikkommission der Medizinischen Fakultät der Universität Würzburg; sequential study number 124/05) and the University of Pittsburgh Cancer Institute (protocol 96-099). All patients provided written informed consent for the collection of samples and subsequent analysis.

Cell culture. Table 1 provides information on the origin and *in vitro* features of the MCC cell lines used in this study. We established four permanently growing cell lines derived from patients with histologically confirmed MCC (BroLi, WaGa, MS-1, and MaTi). BroLi, WaGa, MS-1, MKL-1 (40), and MKL-2 (42a) were positive for MCV DNA by PCR. Clonal integration of the MCV genome was confirmed by Southern blotting for MKL-1, MKL-2, and MS-1 (data not shown). UISO (35), MCC13 (27), and MaTi are MCV-negative MCC cell lines. FM88 is a melanoma cell line (3), and Jurkat (16) is a T-cell line. All cell lines were grown in RPMI 1640 supplemented with 10% fetal bovine serum (FBS) (except for MS-1 at 20% FBS), 100 U/ml penicillin, and 0.1 mg/ml streptomycin. For lentiviral infections, cell counting, or flow cytometric analysis MKL-1, MKL-2, BroLi, MS-1, and MaTi cells were dissociated by incubation in a trypsin–EDTA solution.

Immunoblotting. Cells were lysed in protein extraction buffer (either 1% NP-40, 0.5% sodium deoxycholate, 0.1% sodium dodecyl sulfate [SDS], 150 mM NaCl, and 50 mM Tris-HCl [pH 8.0] or 0.6% SDS, 1 mM EDTA, 10 mM Tris-HCl [pH 8.0], 2 mM NaF, and 2 mM $NaVO_3$) supplemented with a protease inhibitor cocktail (Roche Diagnostics). Samples were resolved by SDS-polyacrylamide gel electrophoresis and were transferred to nitrocellulose membranes. Following 1 h of blocking with Tris-buffered saline (TBS) containing 0.05% Tween 20 and 5% powdered skim milk, membranes were incubated overnight with a primary antibody, washed three times with TBS with 0.05% Tween 20 (TBS-T), and then incubated with a peroxidase-coupled secondary antibody. Bands were detected using a Western Lightning Plus-ECL chemiluminescence detection kit (Perkin-Elmer). To detect MCV TA proteins, monoclonal antibodies CM2B4, recognizing MCV LT (39), and CM8E6, recognizing both the LT and sT proteins (25), were used as reported previously. Rabbit polyclonal antibodies to cleaved poly(ADP-ribose) polymerase (PARP), cleaved caspase-3, cleaved caspase-9, Bcl-2, phospho-Bcl-2 (Ser70), phospho-Bcl-2 (Ser56), Bcl-xL, Mcl-1, Bad, phospho-Bad (Ser112), Bax, Bik, Bim, Bmf, and Puma (Cell Signaling) and a mouse monoclonal antibody to p53 DO-1 (Santa Cruz) were used at 1:1,000. As an internal control, a monoclonal antibody to α-tubulin was used at 1:2,500.

shRNA constructs and lentiviral infection. For the green fluorescent protein (GFP)-selectable knockdown system, a shRNA sequence (sense strand, 5′-GAT CCA CAA GCT CAG AAG TGA CTT CTC TAT TCA AGA GAT AGA GAA GTC ACT TCT GAG CTT GTG GAT TTT TTT G-3′) designed to target nucleotides 391 to 419 (GenBank accession number EU375803) present in all 4 T-antigen mRNAs was cloned into the lentiviral vector KH1 (43) by using SmaI-XbaI sites to generate TA.GFP. For control purposes, a scrambled KH1 shRNA construct provided by Monique Verhaegen (43) was used. For the puromycin-selectable knockdown system, shRNA sequences designed to target nucleotides 222 to 242 (sense strand, 5′-CCG GAA GAG AGG CTC TCT GCA AGC TCT CGA GAG CTT GCA GAG AGC CTC TCT TTT TTG-3′) and nucleotides 173 to 193 (sense strand, 5′-CCG GAA CTC CTT CTG CAT ATA GAC ATC AAG AGT GTC TAT ATG CAG AAG GAG TTT TTT TG-3′) were individually cloned at AgeI and EcoRI sites of the pLKO.1 lentiviral vector to generate T1.puro and T2.puro, respectively. The control plasmid pLKO.1, which has a scrambled nontargeting short hairpin RNA sequence, was obtained from Addgene. Lentiviruses for the KH1 GFP constructs were produced in HEK293T cells using pRSV rev, pHCMV-G, and pMDLg/pRRE helper constructs. Lentiviruses for the puromycin pLKO constructs were produced in HEK293FT cells (Invitrogen) using pPax2 and pMD2.G helper constructs. Two or 3 days following transfection, virus supernatants were harvested and filtered through 0.45-μm-pore-size filters. For infection, virus-containing supernatants were supplemented with 1 μg/ml Polybrene and were then added to the target cells for 4 h (WaGa cells, which are sensitive to Polybrene) or overnight (other cell lines). Following incubation with virus, cells were washed twice with medium. Since KH1 also encodes GFP, the infection rate could be determined by flow cytometry (FACScanto; BD Biosciences). Equal virus titers for TA shRNA and the scrambled viruses were ensured by serial dilutions of the viruses applied to MCC13 cells, giving equal infection efficiencies as measured on day 4 following infection. Infectious titers for puromycin-selectable shRNA vectors determined in UISO cells ranged from 5×10^{-6} to 20×10^{-6} CFU/ml. This indicates that growth failure in MCV-positive cell lines is not due to a low titer of shRNA virus. In order to improve infection rates, it was necessary to dissociate spheroidal growing cells as well as to include 1 μg/ml Polybrene; both measures are accompanied by some degree of death of MCC cells, as indicated by a major sub-G_1 population on day 7 after infection with Sc.GFP (see Fig. 6B).

GFP assay. GFP expression by KH1-infected cells was used to compare the behavior of infected and uninfected cells: on day 1 following infection, the cells were mixed with approximately 20% Polybrene (1 μg/ml)-treated, uninfected

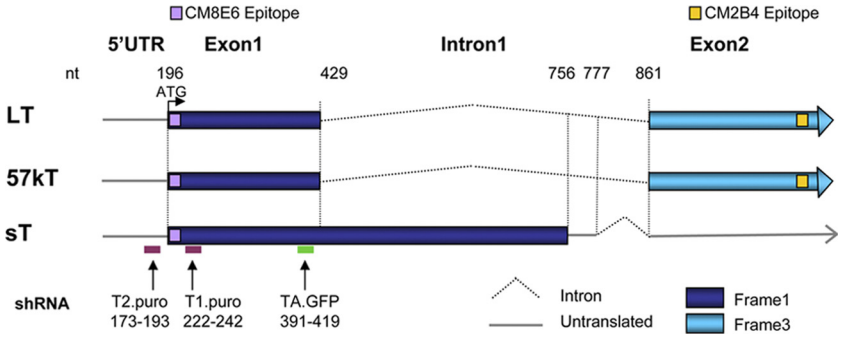

FIG. 1. Structure of the exon 1 and exon 2 junctions for MCV T-antigen mRNAs. The large T (LT) and 57kT proteins are identically encoded by exon 1 and exon 2 but differ due to downstream alternative splicing in exon 2 (not shown). sT translation extends beyond the LT/57kT exon 1 donor site but does not include exon 2. Antibody CM8E6 recognizes all TAs, whereas CM2B4 detects only the LT and 57kT proteins encoded by exon 2. The sequences targeted by the three TA shRNAs used in this study are located within shared regions of exon 1 and are anticipated to target all TA isoforms.

cells. Starting from day 4 postinfection, the frequency of GFP-positive cells in this mixture was determined in a time course.

Cell proliferation and cell viability analyses. At 48 h after lentiviral infection, 10^4 infected UISO or MCC13 cells or 2.5×10^4 infected cells from MCV-positive cell lines (MKL-1, MKL-2, WaGa, and MS-1) were seeded in 96-well plates with 150 μl growth medium containing puromycin (1 μg/ml). From day 3 postinfection, the growth was monitored in the presence of puromycin using the WST-1 assay reagent (Roche) according to the instruction manual. Due to the low efficiency of lentiviral infection in WaGa cells, the proliferation assay was performed after puromycin selection starting at day 6 postinfection. WST-1 is a tetrazolium salt that, when in contact with metabolically active cells, is cleaved to formazan by mitochondrial dehydrogenases. MTS [3-(4,5-dimethylthiazol-2-yl)-5-(3-carboxymethoxyphenyl)-2-(4-sulfophenyl)-2H-tetrazolium] is a similar tetrazolium reagent that can be used to determine the metabolic activity in cell cultures. The MTS assay (Promega) was used for Sc.GFP- and TA.GFP-infected cells, which contained at least 80% infected GFP-positive cells on day 4 postinfection and were not subjected to any kind of selection.

Annexin V assay. The annexin V-phycoerythrin (PE) apoptosis detection kit I (BD Pharmingen, San Diego, CA) was used to identify apoptotic cells by flow cytometry. According to the manufacturer's instructions, the cells were double stained with PE-labeled annexin V and the DNA-intercalating agent 7-aminoactinomycin D (7-AAD). Analysis was performed on a FACSCanto flow cytometer (BD Biosciences, Heidelberg, Germany). In order to analyze the infected cells exclusively, they were gated on GFP. Subsequently, the early apoptotic cells were identified as the 7-AAD^- annexin V^+ cells.

Cell cycle analysis. To determine the proportion of cells in different phases of the cell cycle, analysis of cellular DNA content was performed. Dissociated single cells were pelleted and resuspended in 0.5 ml phosphate-buffered saline (PBS) supplemented with 1% fetal calf serum. Five milliliters of ice-cold ethanol (100%) was added, followed by overnight incubation at 4°C. Fixed cells were pelleted; resuspended in 1 ml PBS supplemented with 1% fetal calf serum, 0.05 mg/ml propidium iodide (PI), and 0.1 mg/ml RNase A; and incubated for 1 h at 37°C. Analysis was performed on a FACSCanto flow cytometer. For bromodeoxyuridine (BrdU) incorporation, MCV-positive cell lines were infected with the lentiviral shRNA vector Sc.puro or T1.puro. To eliminate uninfected cells, puromycin (1 μg/ml) was added to the culture medium for 4 days starting at day 2 postinfection. At day 8 postinfection, cells were labeled with 10 μM BrdU for 3 h. BrdU incorporation was assayed using an anti-BrdU monoclonal antibody (BD Biosciences), followed by PI staining as described above. Dead cells were gated out in this assay.

Statistical analysis. Statistical analysis (by the Mann-Whitney test) was performed using GraphPad Prism software (GraphPad Software, La Jolla, CA).

RESULTS

Expression of MCV T antigen in MCV-positive MCC cell lines. The MCV TA locus expresses alternatively spliced transcripts encoding the LT, sT, and 57kT proteins (39, 40), which share an identical N-terminal amino acid sequence encoded by exon 1 of LT (Fig. 1). We examined MCV TA expression in a panel of established MCV-positive (MKL-1 and MKL-2 [42a, 40]) and MCV-negative (UISO [35] and MCC-13 [27]) MCC cell lines, as well as in four newly established MCC cell lines (BroLi, MaTi, WaGA, and MS-1). WaGa, BroLi, and MS-1 are positive for MCV DNA, whereas MaTi is negative (Table 1).

Immunoblotting for an exon 2 epitope with antibody CM2B4 confirmed LT protein expression in MKL-1, MKL-2, BroLi, WaGa, and MS-1 cells (Fig. 2A). LT bands range in size from 40 kDa (MKL-2) to 60 kDa (MS-1), consistent with the different tumor-derived truncating LT mutations that were determined for these cell lines (Table 1). However, the apparent molecular weights are higher than the predicted molecular weights, and several cell lines (MKL-1, BroLi, and WaGa) show multiple LT bands, suggesting posttranslational LT modification and aberrant splicing events. Similar LT banding patterns were replicated by immunoblotting with CM8E6 (Fig. 2B), a monoclonal antibody recognizing an exon 1 epitope common to all TA isoforms, including the sT protein (18 kDa), which is not affected by truncating mutations (Fig. 1). MCV-negative UISO, MCC13, and MaTi cells do not express any MCV TA isoforms, although a prominent nonspecific signal is present at 75 kDa in all cell lines immunoblotted with antibody CM8E6.

Knockdown of T antigen interferes with the proliferation and survival of MCV-positive MCC cells. To determine if MCV TA expression is required for MCV-positive cell line survival, two independent strategies to knock down all TA mRNAs by targeting exon 1 were developed; the results of these experiments were mutually confirmatory. Locations of knockdown targeting sequences are shown in Fig. 1. The first strategy targeted MCV TA exon 1 using the shRNA lentiviral vector KH1, which also encodes green fluorescent protein (shTA.GFP) (43). Flow cytometry analysis of cells infected with shTA.GFP or its scrambled control (shSc.GFP) virus demonstrated general infection rates ranging from 75 to 95%; one exception, however, was the MCV-negative cell line MaTi, in which less than 50% of cells were infectible. In the second approach, puromycin-selectable lentiviral shRNA vectors (shT1.puro and shT2.puro), which allowed for enrichment of infected cells prior to further analysis, were used. Immunoblotting confirmed the efficient knockdown of LT and sT protein

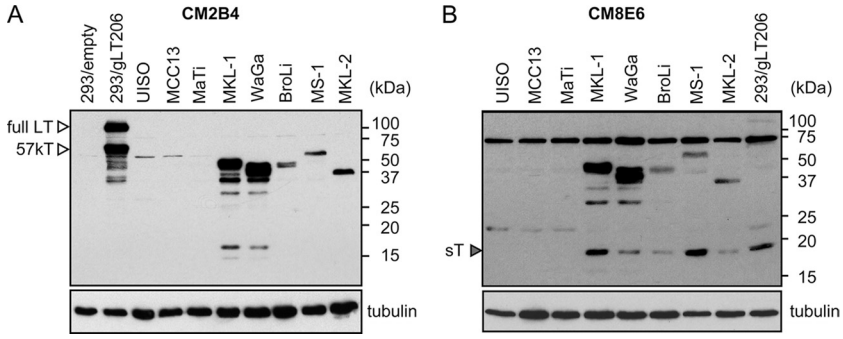

FIG. 2. T-antigen expression in MCC cell lines. Total-cell lysates of the indicated cell lines were analyzed by immunoblotting with antibodies CM2B4 (A) and CM8E6 (B). MCC cell lines MKL-1, WaGa, BroLi, MS-1, and MKL-2 express MCV TAs, whereas UISO, MCC13, and MaTi are negative for MCV infection (nonspecific 60-kDa and 75-kDa bands are also detected by CM2B4 and CM8E6, respectively). LT sizes differ among MCC cell lines and also differ from the size of full-length LT206 expressed in 293 cells, consistent with different carboxyl truncation mutations in different MCV-positive cell lines. Tubulin expression was determined as a protein loading control.

expression in MCV-positive MCC cells by both strategies compared to expression with the respective scrambled controls (Fig. 3A and B).

The impact of shTA.GFP infection on cell growth was analyzed in mixed cultures of infected and uninfected cells (distinguished by the presence or absence of green fluorescence) for the different cell lines. In all 5 MCV-positive cell lines (MKL-1, WaGa, BroLi, MKL-2, and MS-1), a gradual loss of green fluorescent cells was observed over time with shTA.GFP infection, but not with shSc.GFP infection (Fig. 4A). This is consistent with decreased proliferation and/or survival upon TA knockdown. MTS assays performed on MCV-positive shTA.GFP-infected cells confirmed the decrease in metabolic activity 8 to 15 days after infection compared with the activity of cells infected with shSc.GFP (data not shown). In contrast, none of the 5 MCV-negative cell lines (MCC13, MaTi, UISO, FM88, and Jurkat) infected with shTA.GFP or shSc.GFP showed a decrease in cell proliferation over time, as indicated by stable ratios of green fluorescent to nonfluorescent cells (Fig. 4A).

A proliferation assay applying the tetrazolium compound Wst-1 was used to assess the fate of cells infected with puromycin-selectable vectors. Consistent with the results of GFP lentivirus knockdown experiments, MCV-positive MKL-1, WaGa, MKL-2, and MS-1 cells infected with shT1.puro or shT2.puro failed to grow (Fig. 4B), while cells of the MCV-negative cell lines UISO (Fig. 4B) and MCC13 (data not shown) proliferated with kinetics similar to that of the respective shSc.puro-infected controls. In an attempt to differentiate between sT and LT effects, two different shRNA viruses targeting the TA intron 1 region were tested (Fig. 1). Both failed to suppress sT expression; therefore, we cannot distinguish LT from sT effects, although experiments to dissect the contributions of each of these isoforms to cell survival are ongoing.

T-antigen loss results in caspase-independent cell death and cell cycle arrest. To distinguish between induction of cell death

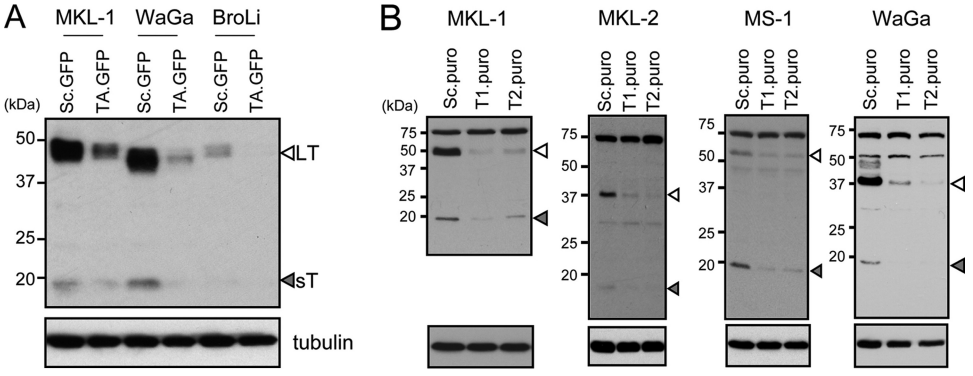

FIG. 3. Knockdown of T-antigen expression using green fluorescent protein (GFP)-expressing and puromycin-selectable lentiviral shRNA vectors. Total-cell lysates were analyzed for LT (open arrowhead) and sT (filled arrowhead) expression by immunoblotting using antibody CM8E6. (A) The indicated MCC cell lines were infected with the lentiviral shRNA vector KH1, encoding GFP and either a shRNA targeting all MCV TA mRNAs (TA.GFP) or a scrambled shRNA (Sc.GFP). The infection rates in this particular experiment were determined to be 79% (MKL-1 TA.GFP), 91% (WaGa TA.GFP), and 81% (BroLi TA.GFP). Knockdown was examined at day 5 postinfection. (B) The indicated MCC cell lines were infected with the lentiviral shRNA vector pLKO, encoding puromycin resistance and either a shRNA targeting all MCV TA mRNAs (T1.puro and T2.puro) or a scrambled shRNA (Sc.puro). To eliminate uninfected cells, puromycin (1 μg/ml) was added to the culture medium at day 2 after infection, and infected cells were selected for 4 days. Knockdown was examined at day 6 postinfection for MKL-1, MKL-2, and MS-1 cells and at day 10 for WaGa cells.

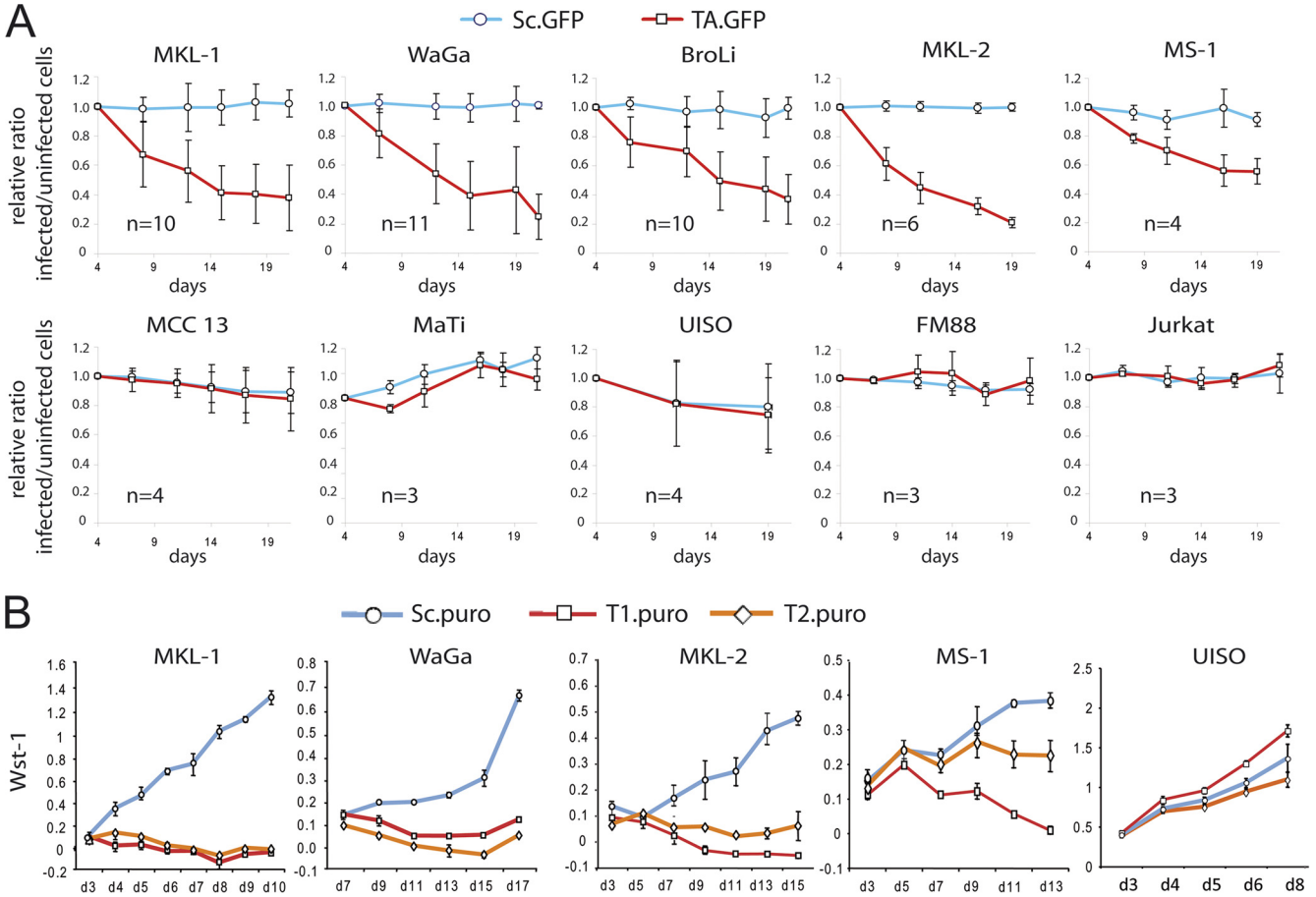

FIG. 4. Altered growth properties of MCV-positive MCC cell lines upon T-antigen knockdown. (A) The indicated cell lines were infected with the lentiviral shRNA vector KH1, encoding GFP and either a shRNA targeting all MCV TA mRNAs (TA.GFP) or a scrambled shRNA (Sc.GFP); infected cells show green fluorescence. To examine altered growth properties upon TA knockdown, the infected, green fluorescent cells were mixed with uninfected, nonfluorescent cells on day 1 postinfection; subsequently, changes in the ratio of green fluorescent to nonfluorescent cells were measured over time. The ratios on day 4 were set to 1. The upper row shows results for MCV-positive cell lines (MKL-1, WaGa, BroLi, MKL-2, and MS-1), and the lower row shows those for MCV-negative cell lines (MCC13, MaTi, UISO, FM88, and Jurkat). Each graph represents mean values (± standard deviations) for at least three independent experiments. The exact number of independent experiments is indicated. (B) The indicated cell lines were infected with the lentiviral shRNA vector pLKO, encoding puromycin and either a shRNA targeting all MCV TA mRNAs (T1.puro and T2.puro) or a scrambled shRNA (Sc.puro). At 48 h after infection, 2.5×10^4 infected MCV-positive cells (MKL-1, MKL-2, and MS-1) and 10^4 infected MCV-negative UISO cells were seeded, and growth was monitored over time in the presence of puromycin (1 μg/ml). For the WaGa cell line, 2.5×10^4 cells were seeded at day 8 postinfection after puromycin selection. The growth properties of the shRNA infected cells were measured by the Wst-1 assay.

and reduced proliferation, we performed annexin V staining and cell cycle analysis. On day 7 after infection with shTA.GFP, TA knockdown in GFP-positive MKL-1 and BroLi cells was associated with a small but distinct fraction of cells (6%) displaying early apoptotic features (7-AAD$^-$ annexin V$^+$ cells) (Fig. 5A). For WaGa cells, we did not observe a significant increase in 7-AAD$^-$ annexin V$^+$ early apoptotic cells upon T-antigen knockdown (Fig. 5A). To study the involvement of apoptosis, we examined caspase activation. shTA.GFP-induced TA knockdown did not increase the cleavage of PARP, caspase-3, or caspase-9 (Fig. 5B). As a control, cleaved forms of caspases as well as PARP protein were generated after doxorubicin treatment, indicating intact caspase-initiated apoptotic pathways in MCC cells (Fig. 5B). Comparable results were obtained by analysis of shT1.puro-infected MCC cells (data not shown).

All MCC cell lines are characterized by a prominent cell fraction in G_0/G_1 (e.g., 85% of MKL-1 cells, 83% of WaGa cells, and 88% of BroLi cells) under standard cell culture conditions. Subsequent to shTA.GFP knockdown, but not after infection with the shSc.GFP control construct, the numbers of WaGa cells in S and G_2/M are reduced (Fig. 6A and B), an effect that is present but less pronounced for MKL-1 and BroLi cells (Fig. 6A). Accumulation of cells in G_1 is also observed upon TA knockdown by infection of MKL-1, WaGa, MKL-2, and MS-1 cells with shT1.puro (Fig. 6C and data not shown). Moreover, decreased BrdU labeling of these cells is indicative of reduced S-phase entry from G_0/G1. (Fig. 6C).

T-antigen knockdown-induced cell death/growth arrest is independent of Bcl-2 family regulators and p53. To investigate the mechanism for decreased MCV-positive cell survival after

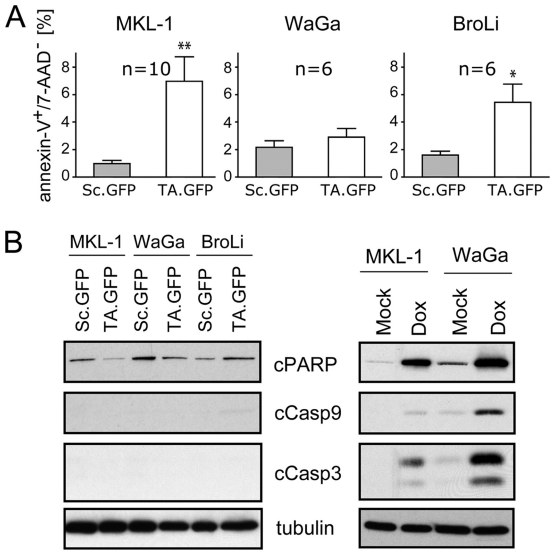

FIG. 5. Induction of cell death but lack of caspase activation upon T-antigen knockdown. The indicated MCC cells were infected with the indicated lentiviral constructs expressing either a shRNA targeting all MCV TA mRNAs (TA.GFP) or a scrambled shRNA (Sc.GFP). (A) Cells were subjected to double staining with annexin V and 7-AAD on day 7 postinfection; to restrict measurements to living, infected cells, only green fluorescent cells were analyzed. The early apoptotic cells are identified as the 7-AAD$^-$ annexin V$^+$ cells. Each bar represents the mean value (+ standard error) for the indicated number of independent experiments. Statistical analysis was done using the Mann-Whitney test (*, $P < 0.05$; **, $P < 0.005$). (B) Immunoblot analysis for cleaved PARP, caspase 9, and caspase 3 proteins in total-cell lysates from the indicated cells on day 5 post-shRNA infection. The induction of cleaved PARP and caspase proteins after a 16-h doxorubicin (1.0 μM) treatment demonstrates that functional apoptotic pathways remain intact in these cell lines.

TA knockdown, we examined expression levels for a panel of pro- and antiapoptotic proteins, i.e., p53, Bad, Bax, Bik, Bim, Bmf, Puma, Bcl-2, Bcl-xL, and Mcl-1 (Fig. 7).

Modest increases in Bcl-xL and Bax levels were observed upon TA knockdown in MKL-1 cells (Fig. 7A and B); however, this observation was not consistent with those for other cell lines analyzed (Fig. 7C). p53 protein was detected in all MCC cell lines except MKL-2. While p53 protein levels were marginally decreased in the MCV-positive cell lines MKL-1, MS-1, and WaGa after TA knockdown, we did not observe specific stabilization or activation of p53, suggesting that the p53 pathway is unlikely to cause the observed TA knockdown-induced growth inhibition or cell death (Fig. 7D). Finally, protein expression of Bcl-2, Mcl-1, Bad, Bik, Bim, and Puma was not altered in MKL-1 cells after TA knockdown with shT1.puro or shT2.puro.

DISCUSSION

Approximately 20% of human cancers worldwide have been linked to infection (28). MCV as a new cause for human cancer is particularly difficult to establish because (i) MCC is relatively rare (5), (ii) MCV infection is near-ubiquitous among adults (10, 23, 29, 42), and (iii) not all MCC tumors are infected with the virus (4, 14, 15, 21, 41). Nonetheless, direct detection of viral proteins is strictly associated with and specific for MCC tumors (39). While MCV infection is widespread, MCV-positive MCC patients have markedly higher titers of antibody to late viral antigens than MCV-negative MCC patients, consistent with persistent antigen stimulation (29, 42). Finally, clonal MCV integration and the presence of specific TA mutations for tumor-derived MCV provide unambiguous evidence that MCV was present prior to tumor cell genesis and that the virus is not an incidental or passenger infection (14, 37).

Analysis of MCC tumors revealed a strong selective pressure within tumors to silence independent DNA replication from the integrated viral genomes in MCC cancer cells. MCV LT encodes carboxyl-terminal origin-binding and helicase domains that are required for viral DNA replication (25, 31), but most MCC-derived MCV LT DNA sequences harbor stop codon mutations truncating these domains (40). These tumor-specific mutations do not affect amino-terminal Rb1 interaction and DnaJ domains, although they may eliminate a putative p53-binding domain. The MCV sT protein, encoded by an alternative reading frame 5′ to the hypermutable LT region, remains unaffected by tumor-specific mutations.

The observational evidence for MCV causality in MCC is directly supported by the experimental studies presented. By means of shRNA knockdown, we demonstrate that MCV-positive MCC cell lines are "addicted" to expression of the viral TAs. We achieved efficient TA knockdown in five different MCV-positive MCC cell lines, using three different exon 1 target sequences and two independent selection methods in order to rule out off-target effects or artifacts due to the method used. In each case, MCV-positive cells initiated growth arrest and/or underwent cell death with the TA exon 1-specific vectors but not with scrambled shRNA vectors. MCV-negative cell lines, however, were unaffected by MCV TA-targeting shRNA, further indicating that this is not likely to be an off-target effect. These results show that MCV TA is required for MCC cell survival among those tumors infected with the virus. Since exon 1 is common to all TA isoforms, all early MCV transcripts were inhibited in our study. Dissecting the contributions of each TA isoform (e.g., LT, sT, and 57kT) to the transformed MCC phenotype will be important for future investigations.

The dependency of the transformed phenotype on the expression of TAs has been shown to be time dependent. In transgenic mice with inducible expression of SV40 TAs in the submandibular gland, hyperplasia was reversed upon the silencing of TA expression after 4 months but persisted when expression was shut down after 7 months (12). Similarly, adenovirus-transformed hamster cells have been reported to lose the previously integrated transforming viral DNA while retaining the oncogenic phenotype (30). It is conceivable that such a phenomenon may also apply to some of the MCV-negative cases of MCC; however, for MCV-positive cell lines, we show clear dependence on MCV TA expression.

Since cell death induced by TA knockdown is not associated with caspase activation, PARP cleavage, major shifts in phosphatidylserine location, or alterations in p53 or Bcl-2 family protein expression, it lacks important features of classical apoptosis. Alternatively, cell death may occur through autophagy, a process of cellular self-degradation involving the lysosomal machinery that has recently attracted increasing attention in cancer research (6). Necrosis, a process distinct from

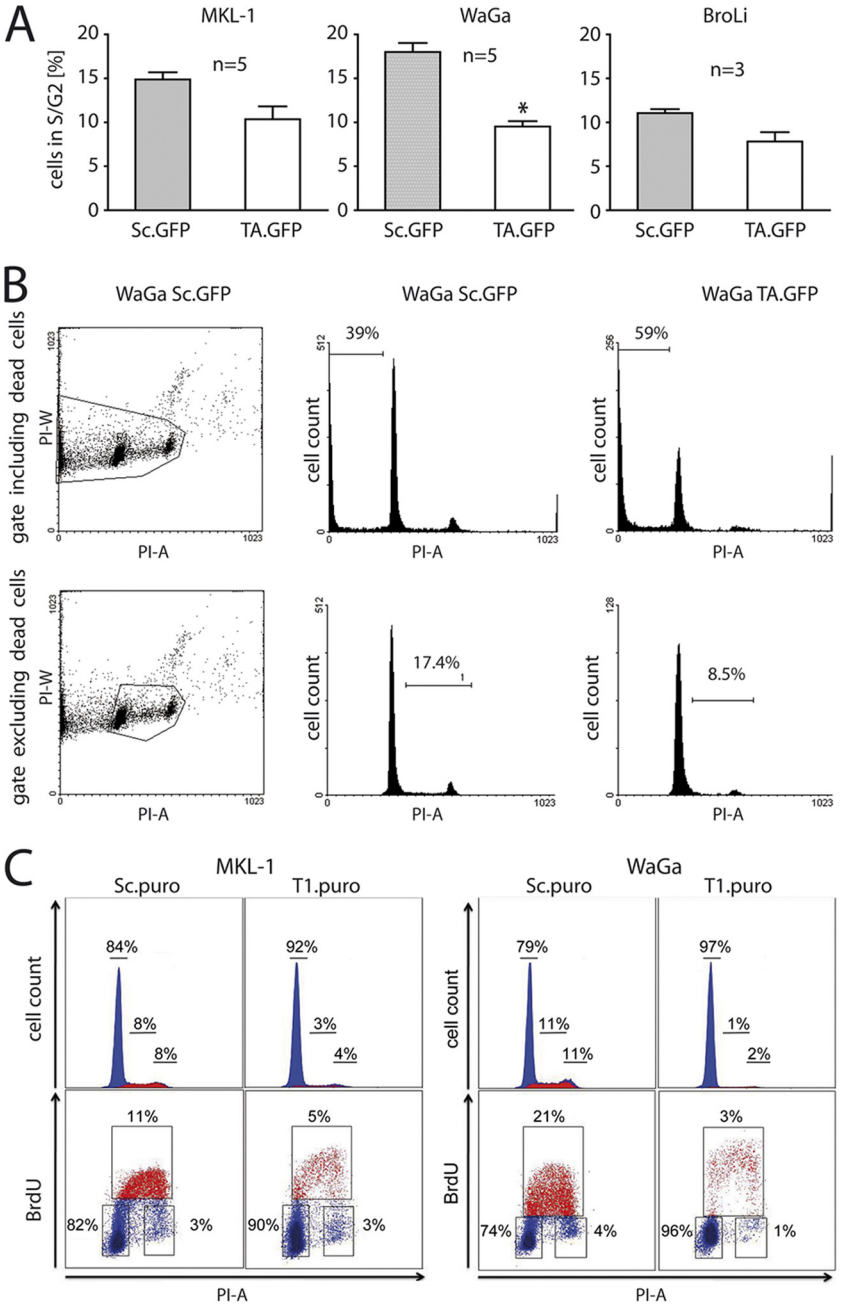

FIG. 6. Decreased cell cycle progression upon T-antigen knockdown in MCV-positive MCC cells. (A) Cells were infected with the indicated lentiviral constructs expressing either a shRNA targeting all MCV TA mRNAs (TA.GFP) or a scrambled shRNA (Sc.GFP). The cellular DNA content was determined by PI staining of fixed cells. The percentage of cells with >2N DNA content on day 7 following infection with Sc.GFP or TA.GFP is given. Each bar represents the mean value (+ standard error) for the indicated number of independent experiments. Statistical analysis was done using the Mann-Whitney test (*, $P < 0.05$). (B) The two PI-A/PI-W dot blots demonstrate the gating strategy used to exclude cellular doublets or doublets and dead sub-G_1 cells. Note the large sub-G_1 fraction that is also visible in the histogram blots of Sc.GFP-infected cells. The percentages of cells in the S and G_2 phases of the cell cycle were estimated in histogram blots after exclusion of the doublets and sub-G_1 cells. (C) MKL-1 or WaGa cells infected with Sc.puro or T1.puro were labeled with 10 μM BrdU for 3 h at day 8 postinfection. BrdU incorporated into the cellular DNA was stained with an anti-BrdU monoclonal antibody followed by PI staining. BrdU-positive cell populations (red) are merged to the cell cycle profile.

either apoptosis or autophagy, may also cause cell death (for a review, see reference 24). The observed cell cycle arrest upon T-antigen knockdown can be more directly explained by alterations of the Rb–E2F pathway: Rb family proteins are the master regulators of S-phase entry, and they are the prominent cellular targets for polyomavirus T antigens (13, 45).

Despite the fact that MCV was discovered only recently, both observational data and the experimental studies described

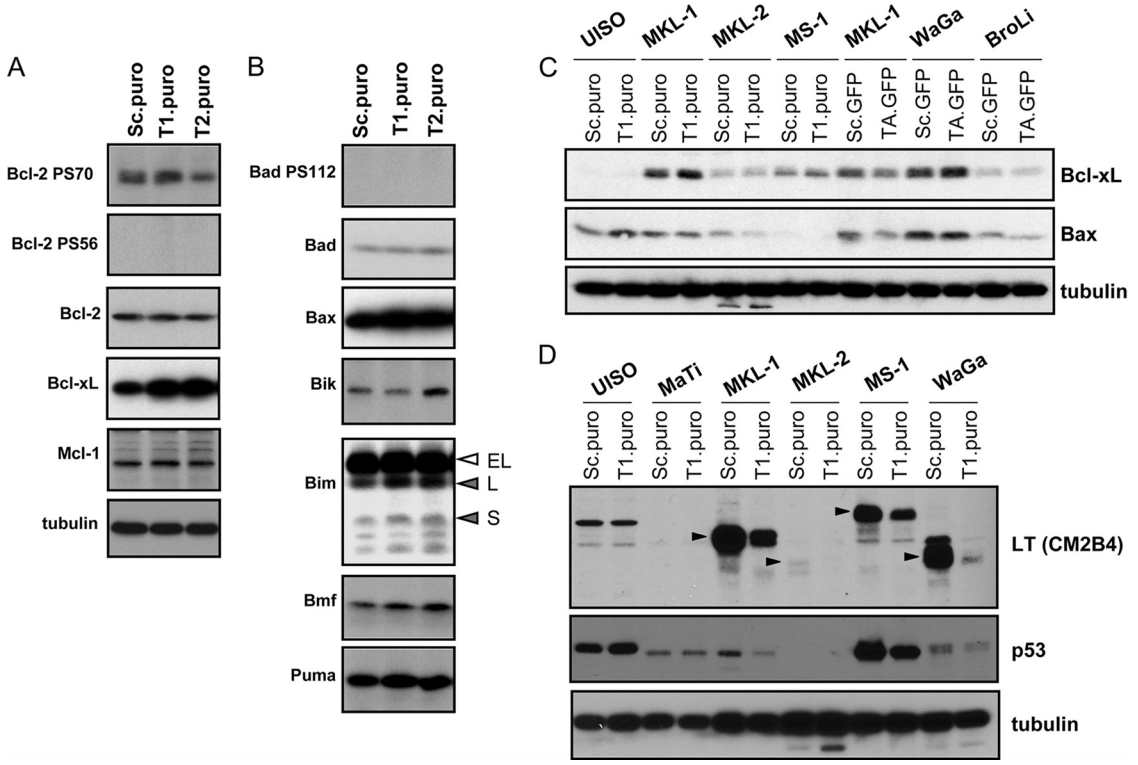

FIG. 7. Bcl-2 family protein expression and phosphorylation and p53 expression after T-antigen knockdown in MCV-positive MCC cells. Total-cell lysates derived from cells on day 6 following infection with either a scrambled shRNA (Sc.puro or Sc.GFP) or a TA-directed shRNA construct (T1.puro, T2.puro, or TA.GFP) were analyzed by immunoblotting. (A and B) The expression of antiapoptotic (A) and proapoptotic (B) Bcl-2 family members is exemplified for MKL-1 cells. (C) Differential Bcl-xL and Bax expression upon TA knockdown with respect to cell line and knockdown strategy. (D) Total p53 protein was analyzed in MCC cell lines infected with Sc.puro or T1.puro. Filled arrowheads indicate truncated LT proteins.

here demonstrate that it is the likely infectious trigger for most human MCC. While polyomaviruses have been studied extensively in animal cancer models, MCV is the first polyomavirus for which strong evidence supports a causal role in human cancer (32). Identifying specific cellular pathways targeted by putative MCV TA oncoproteins can lead directly to new, more effective, and less toxic therapies for this human cancer.

ACKNOWLEDGMENTS

We are grateful to Monique Verhaegen for the KH1 and the KH1-scrambled constructs, to Akio Soeda for providing antibodies, to John Kirkwood for access to Merkel cell tumors through the University of Pittsburgh Cancer Institute Skin Cancer SPORE, to Stefan Gaubatz for critical discussions, and to Billy Bang and Frank Lowe for help with the manuscript.

J. C. Becker was supported by the DFG (KFO124), and R. Houben was supported by the Wilhelm-Sander Stiftung (grant 2007.057.1) and the IZKF Würzburg (B157). This work was supported by NIH CA136363 and CA120726, the Al Copeland Foundation, and University of Pittsburgh EXPLORER grants to P. S. Moore and Y. Chang, who are American Cancer Society Research Professors.

REFERENCES

1. **Ahuja, D., M. T. Saenz-Robles, and J. M. Pipas.** 2005. SV40 large T antigen targets multiple cellular pathways to elicit cellular transformation. Oncogene **24:**7729–7745.
2. **Arroyo, J. D., and W. C. Hahn.** 2005. Involvement of PP2A in viral and cellular transformation. Oncogene **24:**7746–7755.
3. **Bakker, A. B. H., J. H. Phillips, C. G. Figdor, and L. L. Lanier.** 1998. Killer cell inhibitory receptors for MHC class I molecules regulate lysis of melanoma cells mediated by NK cells, γδ T cells, and antigen-specific CTL. J. Immunol. **160:**5239–5245.
4. **Becker, J. C., R. Houben, S. Ugurel, U. Trefzer, C. Pfohler, and D. Schrama.** 2009. MC polyomavirus is frequently present in Merkel cell carcinoma of European patients. J. Investig. Dermatol. **129:**248–250.
5. **Becker, J. C., D. Schrama, and R. Houben.** 2009. Merkel cell carcinoma. Cell. Mol. Life Sci. **66:**1–8.
6. **Brech, A., T. Ahlquist, R. A. Lothe, and H. Stenmark.** 2009. Autophagy in tumour suppression and promotion. Mol. Oncol. **3:**366–375.
7. **Busam, K. J., A. A. Jungbluth, N. Rekthman, D. Coit, M. Pulitzer, J. Bini, R. Arora, N. C. Hanson, J. A. Tassello, D. Frosina, P. Moore, and Y. Chang.** 2009. Merkel cell polyomavirus expression in Merkel cell carcinomas and its absence in combined tumors and pulmonary neuroendocrine carcinomas. Am. J. Surg. Pathol. **33:**1378–1385.
8. **Carter, J. J., K. G. Paulson, G. C. Wipf, D. Miranda, M. M. Madeleine, L. G. Johnson, B. D. Lemos, S. Lee, A. H. Warcola, J. G. Iyer, P. Nghiem, and D. A. Galloway.** 2009. Association of Merkel cell polyomavirus-specific antibodies with Merkel cell carcinoma. J. Natl. Cancer Inst. **101:**1510–1522.
9. **Chang, Y., E. Cesarman, M. S. Pessin, F. Lee, J. Culpepper, D. M. Knowles, and P. S. Moore.** 1994. Identification of herpesvirus-like DNA sequences in AIDS-associated Kaposi's sarcoma. Science **266:**1865–1869.
10. **Cheng, J., J. A. DeCaprio, M. M. Fluck, and B. S. Schaffhausen.** 2009. Cellular transformation by simian virus 40 and murine polyoma virus T antigens. Semin. Cancer Biol. **19:**218–228.
11. **Engels, E. A., M. Frisch, J. J. Goedert, R. J. Biggar, and R. W. Miller.** 2002. Merkel cell carcinoma and HIV infection. Lancet **359:**497–498.
12. **Ewald, D., M. Li, S. Efrat, G. Auer, R. J. Wall, P. A. Furth, and L. Hennighausen.** 1996. Time-sensitive reversal of hyperplasia in transgenic mice expressing SV40 T antigen. Science **273:**1384–1386.
13. **Felsani, A., A. M. Mileo, and M. G. Paggi.** 2006. Retinoblastoma family proteins as key targets of the small DNA virus oncoproteins. Oncogene **25:**5277–5285.
14. **Feng, H., M. Shuda, Y. Chang, and P. S. Moore.** 2008. Clonal integration of a polyomavirus in human Merkel cell carcinoma. Science **319:**1096–1100.
15. **Garneski, K. M., A. H. Warcola, Q. Feng, N. B. Kiviat, J. H. Leonard, and P. Nghiem.** 2009. Merkel cell polyomavirus is more frequently present in

North American than Australian Merkel cell carcinoma tumors. J. Investig. Dermatol. **129:**246–248.
16. **Gillis, S., and J. Watson.** 1980. Biochemical and biological characterization of lymphocyte regulatory molecules. V. Identification of an interleukin 2-producing human leukemia T cell line. J. Exp. Med. **152:**1709–1719.
17. **Heath, M., N. Jaimes, B. Lemos, A. Mostaghimi, L. C. Wang, P. F. Penas, and P. Nghiem.** 2008. Clinical characteristics of Merkel cell carcinoma at diagnosis in 195 patients: the AEIOU features. J. Am. Acad. Dermatol. **58:**375–381.
18. **Hill, A. B.** 1965. The environment and disease: association or causation? Proc. R. Soc. Med. **58:**295–300.
19. **Hodgson, N. C.** 2005. Merkel cell carcinoma: changing incidence trends. J. Surg. Oncol. **89:**1–4.
20. **Houben, R., D. Schrama, and J. C. Becker.** 2009. Molecular pathogenesis of Merkel cell carcinoma. Exp. Dermatol. **18:**193–198.
21. **Kassem, A., A. Schopflin, C. Diaz, W. Weyers, E. Stickeler, M. Werner, and H. A. Zur.** 2008. Frequent detection of Merkel cell polyomavirus in human Merkel cell carcinomas and identification of a unique deletion in the VP1 gene. Cancer Res. **68:**5009–5013.
22. **Kassem, A., K. Technau, A. K. Kurz, D. Pantulu, M. Loning, G. Kayser, E. Stickeler, W. Weyers, C. Diaz, M. Werner, D. Nashan, and H. A. Zur.** 2009. Merkel cell polyomavirus sequences are frequently detected in nonmelanoma skin cancer of immunosuppressed patients. Int. J. Cancer **125:**356–361.
23. **Kean, J. M., S. Rao, M. Wang, and R. L. Garcea.** 2009. Seroepidemiology of human polyomaviruses. PLoS Pathog. **5:**e1000363.
24. **Kroemer, G., and S. J. Martin.** 2005. Caspase-independent cell death. Nat. Med. **11:**725–730.
25. **Kwun, H. J., A. Guastafierro, M. Shuda, G. Meinke, A. Bohm, P. S. Moore, and Y. Chang.** 2009. The minimum replication origin of Merkel cell polyomavirus has a unique large T-antigen loading architecture and requires small T-antigen expression for optimal replication. J. Virol. **83:**12118–12128.
26. **Lanoy, E., D. Costagliola, and E. A. Engels.** 2010. Skin cancers associated with HIV infection and solid-organ transplantation among elderly adults. Int. J. Cancer **126:**1724–1731.
27. **Leonard, J. H., P. Dash, P. Holland, J. H. Kearsley, and J. R. Bell.** 1995. Characterisation of four Merkel cell carcinoma adherent cell lines. Int. J. Cancer **60:**100–107.
28. **Parkin, D. M.** 2006. The global health burden of infection-associated cancers in the year 2002. Int. J. Cancer **118:**3030–3044.
29. **Pastrana, D. V., Y. L. Tolstov, J. C. Becker, P. S. Moore, Y. Chang, and C. B. Buck.** 2009. Quantitation of human seroresponsiveness to Merkel cell polyomavirus. PLoS Pathog. **5:**e1000578.
30. **Pfeffer, A., R. Schubbert, G. Orend, K. Hilger-Eversheim, and W. Doerfler.** 1999. Integrated viral genomes can be lost from adenovirus type 12-induced hamster tumor cells in a clone-specific, multistep process with retention of the oncogenic phenotype. Virus Res. **59:**113–127.
31. **Pipas, J. M.** 1992. Common and unique features of T antigens encoded by the polyomavirus group. J. Virol. **66:**3979–3985.
32. **Poulin, D. L., and J. A. DeCaprio.** 2006. Is there a role for SV40 in human cancer? J. Clin. Oncol. **24:**4356–4365.
33. **Reisinger, D. M., J. D. Shiffer, A. B. Cognetta, Y. Chang, and P. S. Moore.** Lack of evidence for basal or squamous cell carcinoma infection with Merkel cell polyomavirus in immunocompetent patients with Merkel cell carcinoma. J. Am. Acad. Dermatol., in press.
34. **Ridd, K., S. Yu, and B. C. Bastian.** 2009. The presence of polyomavirus in non-melanoma skin cancer in organ transplant recipients is rare. J. Investig. Dermatol. **129:**250–252.
35. **Ronan, S. G., A. D. Green, A. Shilkaitis, T. S. Huang, and T. K. Das Gupta.** 1993. Merkel cell carcinoma: in vitro and in vivo characteristics of a new cell line. J. Am. Acad. Dermatol. **29:**715–722.
36. Reference deleted.
37. **Sastre-Garau, X., M. Peter, M. F. Avril, H. Laude, J. Couturier, F. Rozenberg, A. Almeida, F. Boitier, A. Carlotti, B. Couturaud, and N. Dupin.** 2009. Merkel cell carcinoma of the skin: pathological and molecular evidence for a causative role of MCV in oncogenesis. J. Pathol. **218:**48–56.
38. **Schaffhausen, B. S., and T. M. Roberts.** 2009. Lessons from polyoma middle T antigen on signaling and transformation: a DNA tumor virus contribution to the war on cancer. Virology **384:**304–316.
39. **Shuda, M., R. Arora, H. J. Kwun, H. Feng, R. Sarid, M. T. Fernandez-Figueras, Y. Tolstov, O. Gjoerup, M. M. Mansukhani, S. H. Swerdlow, P. M. Chaudhary, J. M. Kirkwood, M. A. Nalesnik, J. A. Kant, L. M. Weiss, P. S. Moore, and Y. Chang.** 2009. Human Merkel cell polyomavirus infection I. MCV T antigen expression in Merkel cell carcinoma, lymphoid tissues and lymphoid tumors. Int. J. Cancer **125:**1243–1249.
40. **Shuda, M., H. Feng, H. J. Kwun, S. T. Rosen, O. Gjoerup, P. S. Moore, and Y. Chang.** 2008. T antigen mutations are a human tumor-specific signature for Merkel cell polyomavirus. Proc. Natl. Acad. Sci. U. S. A. **105:**16272–16277.
41. **Sihto, H., H. Kukko, V. Koljonen, R. Sankila, T. Bohling, and H. Joensuu.** 2009. Clinical factors associated with Merkel cell polyomavirus infection in Merkel cell carcinoma. J. Natl. Cancer Inst. **101:**938–945.
42. **Tolstov, Y. L., D. V. Pastrana, H. Feng, J. C. Becker, F. J. Jenkins, S. Moschos, Y. Chang, C. B. Buck, and P. S. Moore.** 2009. Human Merkel cell polyomavirus infection II. MCV is a common human infection that can be detected by conformational capsid epitope immunoassays. Int. J. Cancer **125:**1250–1256.

42a. **Van Gele, M., J. H. Leonard, N. Van Roy, H. Van Limbergen, S. Van Belle, V. Cocquyt, H. Salwen, A. De Paepe, and F. Speleman.** 2002. Combined karyotyping, CGH and M-FISH analysis allows detailed characterization of unidentified chromosomal rearrangements in Merkel cell carcinoma. Int. J. Cancer **101:**137–145.

43. **Verhaegen, M., J. A. Bauer, C. Martín de la Vega, G. Wang, K. G. Wolter, J. C. Brenner, Z. Nikolovska-Coleska, A. Bengtson, R. Nair, J. T. Elder, M. Van Brocklin, T. E. Carey, C. R. Bradford, S. Wang, and M. S. Soengas.** 2006. A novel BH3 mimetic reveals a mitogen-activated protein kinase-dependent mechanism of melanoma cell death controlled by p53 and reactive oxygen species. Cancer Res. **66:**11348–11359.
44. **Wetzels, C. T., J. G. Hoefnagel, J. M. Bakkers, H. B. Dijkman, W. A. Blokx, and W. J. Melchers.** 2009. Ultrastructural proof of polyomavirus in Merkel cell carcinoma tumour cells and its absence in small cell carcinoma of the lung. PLoS One **4:**e4958.
45. **White, M. K., and K. Khalili.** 2006. Interaction of retinoblastoma protein family members with large T-antigen of primate polyomaviruses. Oncogene **25:**5286–5293.
46. **Zerrahn, J., U. Knippschild, T. Winkler, and W. Deppert.** 1993. Independent expression of the transforming amino-terminal domain of SV40 large I antigen from an alternatively spliced third SV40 early mRNA. EMBO J. **12:**4739–4746.